Dyes and Pigments 82 (2009) 31–39

Contents lists available at ScienceDirect

Dyes and Pigments

journal homepage: www.elsevier.com/locate/dyepig

The facile synthesis and optical nonlinearity of hyperbranched polyaspartimides with azobenzene dyes

Cheng-Che Tsai [a], Tsung-Yi Chao [a,**], Hsun-Lien Lin [a], Yue-Hua Liu [a], Huey-Ling Chang [b,**], Ying-Ling Liu [c], Ru-Jong Jeng [a,*]

[a] Department of Chemical Engineering, National Chung Hsing University, 250 Kuo-Kuang Road, Taichung 402, Taiwan
[b] Department of Chemical and Materials Engineering, National Chinyi University of Technology, Taichung 411, Taiwan
[c] Department of Chemical Engineering and R&D Center for Membrane Technology, Chung Yuan Christian University, 200 Chung-Pei Road, Taoyuan 320, Taiwan

ARTICLE INFO

Article history:
Received 3 September 2008
Received in revised form
28 October 2008
Accepted 28 October 2008
Available online 5 November 2008

Keywords:
Azobenzene dye
Hyperbranched polymer
Michael addition reaction
Nonlinear optical
Polyaspartimides
Electro-optical coefficient

ABSTRACT

A series of thermally stable nonlinear optical hyperbranched polyaspartimides were synthesized via the Michael addition reaction of a fluorine-containing trimaleimide, 1,1-tris[4-(4-maleimide-2-trifluoromethyl-phenoxy)-phenyl]ethane and two respective azobenzene dyes, namely bis(4-aminophenyl(4-(4-nitro-phenyl)-diazenyl)phenyl)-amine and 2,4-diamino-4′-(4-nitrophenyl-diazenyl)-azobenzene, using *p*-toluenesulfonic acid as catalyst. The incorporation of fluorine-rich components within the hyperbranched polymers increased solubility in organic solvents and reduced optical loss. Owing to the three-dimensional, void-rich, topological structure of the highly branched polymers, the spatial separation of the dyes endows the polymers with a favorable site isolation effect, which thereby negates chromophoric aggregation. Using *in situ* contact poling, electro-optical coefficients, r_{33} of 6.5–14.7 pm V^{-1} and temporal stability at 80 °C were obtained. Both the dynamic thermal and temporal stabilities of the hyperbranched polyaspartimides were superior to those of their linear analogues.

1. Introduction

Second-order nonlinear optical (NLO) polymeric materials have attracted much attention in the past two decades because of their potential applications in the fields of high-speed electrooptic (EO) modulators, optical data transmission and optical information processing [1,2]. Organic polymers are regarded as potentially useful for these optical devices due to their large optical nonlinearity and ease of fabrication. Polymer scientists have tried to design and synthesize new dyes to produce better optical nonlinearity [3]. Unfortunately, an increasing first hyperpolarizability ($\mu\beta$) is accompanied by a bathochromic shift due to a large π-conjugated length and/or stronger donor and acceptor capacity. Therefore, there is always a tradeoff between optical nonlinearity and transparency [4,5]. Furthermore, a proportional relationship between dye concentration and optical nonlinearity is observed only in low dye contents [6]. In general, intermolecular dipole interactions in large dye contents would cause an obvious decrement of optical nonlinearity. In order to improve the optical nonlinearity, a chemical structure variation is utilized to suppress the dipole interactions [7–9]. Theoretical analyses also suggest that optimization of molecular shape can minimize this intermolecular electrostatic interaction and thus enhance the poling efficiency to some degree [10–12]. Dendrimers possess a spherical shape, and dendritic structures consisting of NLO dyes have been demonstrated to display large EO coefficients due to their site isolation effects [13,14]. However, the dendrimers usually require highly complicated and repetitive synthetic routes. Unlike dendrimers, hyperbranched polymers are easy to synthesize, and yet possess many unusual properties similar to those of the dendrimers. The three-dimensional spatial separation of the dyes endows the polymers with favorable site isolation effects [15–17], and their void-rich topological structure would minimize optical loss in the NLO process [18,19].

In our previous study [20], NLO hyperbranched polymers were synthesized via the ring-opening addition reaction of azetidine-2,4-dione. It was found that the presence of a three-dimensional structure was capable of enhancing EO coefficients. However, thermal properties of the hyperbranched polymers are usually at issue due to the presence of highly branched structures. This poses an important challenge to material scientists apart from the large optical nonlinearity. There are many efficient ways to improve the stability of hyperbranched NLO polymers, including incorporating

* Corresponding author. Tel.: +886 4 22852581; fax: +886 4 22854734.
** Corresponding authors.
E-mail address: rjjeng@nchu.edu.tw (R.-J. Jeng).

0143-7208/$ – see front matter © 2008 Elsevier Ltd. All rights reserved.
doi:10.1016/j.dyepig.2008.10.013

a high glass transition temperature (T_g) and/or crosslinking features [21,22]. Generally, aromatic polyimides have been selected as promising candidates to achieve excellent NLO stability at elevated temperatures because of their high T_gs [23–25]. However, condensation type polyimides usually suffer from processing problems due to their insolubility, infusibility, and evolution of volatiles during imide ring formation. As reported in Refs. [23–30], polyaspartimides, which could be obtained through Michael addition reaction between amine and maleimide compounds, have shown more favorable properties in processing than do the condensation type polyimides.

The hyperbranched polymers are sometimes prepared by facile one-pot self-polymerization of AB_x monomers [31–34]. However, their monomers often involve wearisome multistep organic syntheses [35]. Therefore, A_2 (difunctional monomer) + B_3 (trifunctional monomer) systems are alternatively adopted for the synthesis of hyperbranched polymers [36,37]. Because of this, the '$A_2 + B_3$' approach is taken to synthesize the NLO hyperbranched polyaspartimides via Michael addition reaction between a fluorine-containing trimaleimide and two respective azobenzene dyes, bis(4-aminophenyl(4-(4-nitrophenyl)-diazenyl)-phenyl)amine (DAC) and 2,4-diamino-4′-(4-nitrophenyl-diazenyl)-azobenzene (DNDA), using *p*-toluenesulfonic acid as catalyst. By incorporating fluorine-rich components into the hyperbranched polyaspartimides, an increased solubility and decreased optical loss would be obtained. Therefore, the resulting product would be a rigid hyperbranched system with good optical quality.

2. Experimental

All chemicals were purchased and used as-received unless otherwise stated. All reactions were carried out under nitrogen. The solvents were purified by distillation under reduced pressure over calcium hydride. ^{1}H NMR spectra were obtained with a Varian Gemini-200 using $CDCl_3$ and DMSO-d_6. Infrared spectra were recorded by using a Perkin Elmer Paragon 500 FT-IR Spectrophotometer. Elemental analysis (EA) was performed on an F002 Heraeus CHN-OS Rapid Elemental Analyzer employing acetanilide as a standard. Thermal analyses using a differential scanning calorimeter (DSC) and thermogravimetric analyzer (TGA) were performed under a nitrogen atmosphere (Seiko SII model SSC/5200). A heating rate of 10 °C/min was used. Thermal degradation temperatures (T_ds) were taken at 5% weight loss. T_gs were measured at the second heating of samples. UV–vis spectra were recorded on a Perkin Elmer Lambda 2S spectrophotometer.

2.1. Synthesis of 1,1,1-tris[4-(4-nitro-2-trifluoromethylphenoxy)phenyl]ethane (**1**) (Fig. 1)

Compound 1,1,1-tris-(hydroxyphenyl) ethane (THPE) (0.613 g, 2 mmol) and 2-chloro-5-nitrobenzo-trifluoride [ed. Note: highly toxic; avoid its contact with water] (1.353 g, 6 mmol) were first dissolved in 10 cm^3 DMAc in a 50 cm^3 flask. After the mixture was completely dissolved, potassium carbonate (1.38 g, 10 mmol) was added. The solution was stirred at room temperature for 30 min, and then heated at 125 °C for 15 h. The obtained mixture was poured into acetic acid/water (volume ratio 1/9) to give a white solid, which was collected, washed thoroughly with water, and dried under vacuum at 80 °C. Yield: 92.3%.

$C_{41}H_{24}F_9N_3O_9$ (873.14): Calcd. C 56.37%, H 2.77%, N 4.81%; Found C 56.12%, H 2.91%, N 4.86%.

^{1}H NMR (DMSO-d_6): δ_{ppm} = 7.02–7.48 and 8.23–8.54 (m, Ar–H), 2.23 (s, –CH_3).

IR (KBr): 1046 and 1337 cm^{-1} (–C═O), 3383 and 1340 and 1525 cm^{-1} (–NO_2).

2.2. Synthesis of 1,1,1-tris[4-(4-amino-2-trifluoromethylphenoxy)phenyl] ethane (**2**) (Fig. 1)

A suspension of the purified trinitro compound **1** (1.752 g, 2 mmol), 10% Pd/C (0.45 g) in ethanol (75 cm^3), and hydrazine monohydrate (5 cm^3) was stirred thoroughly. The mixture was heated at reflux temperature for 4 h. Subsequently, the reaction solution was filtered hot to remove Pd/C, and the filtrate was then distilled to remove the solvent. The obtained mixture was poured into water to wash redundant hydrazine monohydrate. The precipitate was white-to-cream-colored crystals after drying in vacuum at room temperature. Yield: 84.7%.

$C_{41}H_{30}F_9N_3O_3$ (783.21): Calcd. C 62.84%, H 3.86%, N 5.36%; Found C 62.52%, H 4.10%, N 5.43%.

^{1}H NMR (DMSO-d_6): δ_{ppm} = 6.41–7.15 (m, Ar–H), 5.44 (s, –NH_2) and 2.03 (s, –CH_3).

IR (KBr): 1046 and 1337 cm^{-1} (–C═O), 3383 and 3467 cm^{-1} (–NH_2).

2.3. Synthesis of 1,1,1-tris[4-(4-maleimide-2-trifluoromethylphenoxy)-phenyl]ethane (trimaleimide; Fig. 1)

Compound **2** (2.35 g, 3 mmol) was first dissolved in 20 cm^3 DMAc in a 100 cm^3 flask. After the mixture was completely dissolved, maleic anhydride (1.08 g, 1.1 mmol) was added. The solution was stirred at room temperature for 12 h, and then acetic anhydride (2.856 g, 2.8 mmol) and sodium acetate (0.41 g, 5 mmol) were added to the solution at 60 °C. The solution was stirred for another 50 min. The product was purified by re-precipitations into water, and dried under vacuum. Yield: 58.2%.

$C_{53}H_{30}F_9N_3O_9$ (1023.18): Calcd. C 62.18%, H 2.95%, N 4.10%; Found C 61.83%, H 3.34%, N 3.94%.

^{1}H NMR ($CDCl_3$): δ_{ppm} = 2.14 (3H, s, –CH_3), 6.81 (6H, s, (maleimide) CH═CH), 6.96–7.11 (15H, m, Ar–H & (Ar–CF_3)–H), 7.39 (3H, d, (Ar–CF_3)–H), 7.60 (3H, s, (Ar–CF_3)–H).

IR (KBr): 827 and 3103 cm^{-1} (═C–H of maleimide), 1320 cm^{-1} (–C–N), 1720 cm^{-1} (–C═O).

FAB MS: *m*/*z* 1023.1 (M^+).

2.4. Synthesis of 1,1-bis[4-(4-nitro-2-trifluoromethylphenoxy)-phenyl]-1-phenylethane (**3**) (Fig. 1)

Two compounds, 4,4-(1-phenylethylidene) (0.29 g, 1 mmol) and 2-chloro-5-nitrobenzo-trifluoride (0.4511 g, 2 mmol) were first dissolved in 20 cm^3 DMAc in a 50 cm^3 flask. After the mixture was completely dissolved, potassium carbonate (0.45 g, 2 mmol) was added to it in one portion. The solution was stirred at room temperature for 30 min, and then heated at 125 °C for 15 h. The obtained mixture was poured into acetic acid/water (volume ratio 1/9) to give a white solid, which was collected, washed thoroughly with water, and dried under vacuum at 80 °C. Yield: 94.1%.

$C_{34}H_{22}F_6N_2O_6$ (668.14): Calcd. C 61.08%, H 3.32%, N 4.19%; Found C 61.22%, H 3.47%, N 4.23%.

^{1}H NMR (DMSO-d_6): δ_{ppm} = 7.02–7.58 and 8.31–8.72 (m, Ar-H), 2.23 (s, –CH_3).

IR (KBr): 1046 and 1337 cm^{-1} (–C═O), 3383 and 1340 and 1525 cm^{-1} (–NO_2).

2.5. Synthesis of 1,1-bis[4-(4-amino-2-trifluoromethylphenoxy)-phenyl]-1-phenylethane (**4**) (Fig. 1)

A suspension of the purified dinitro compound **3** (1.34 g, 2 mmol), 10% Pd/C (0.91 g) in ethanol (180 cm^3), and hydrazine monohydrate (14 cm^3) was stirred thoroughly. The mixture was heated at reflux temperature for 5 h. The reaction solution was filtered hot to remove Pd/C, and the filtrate was then distilled to

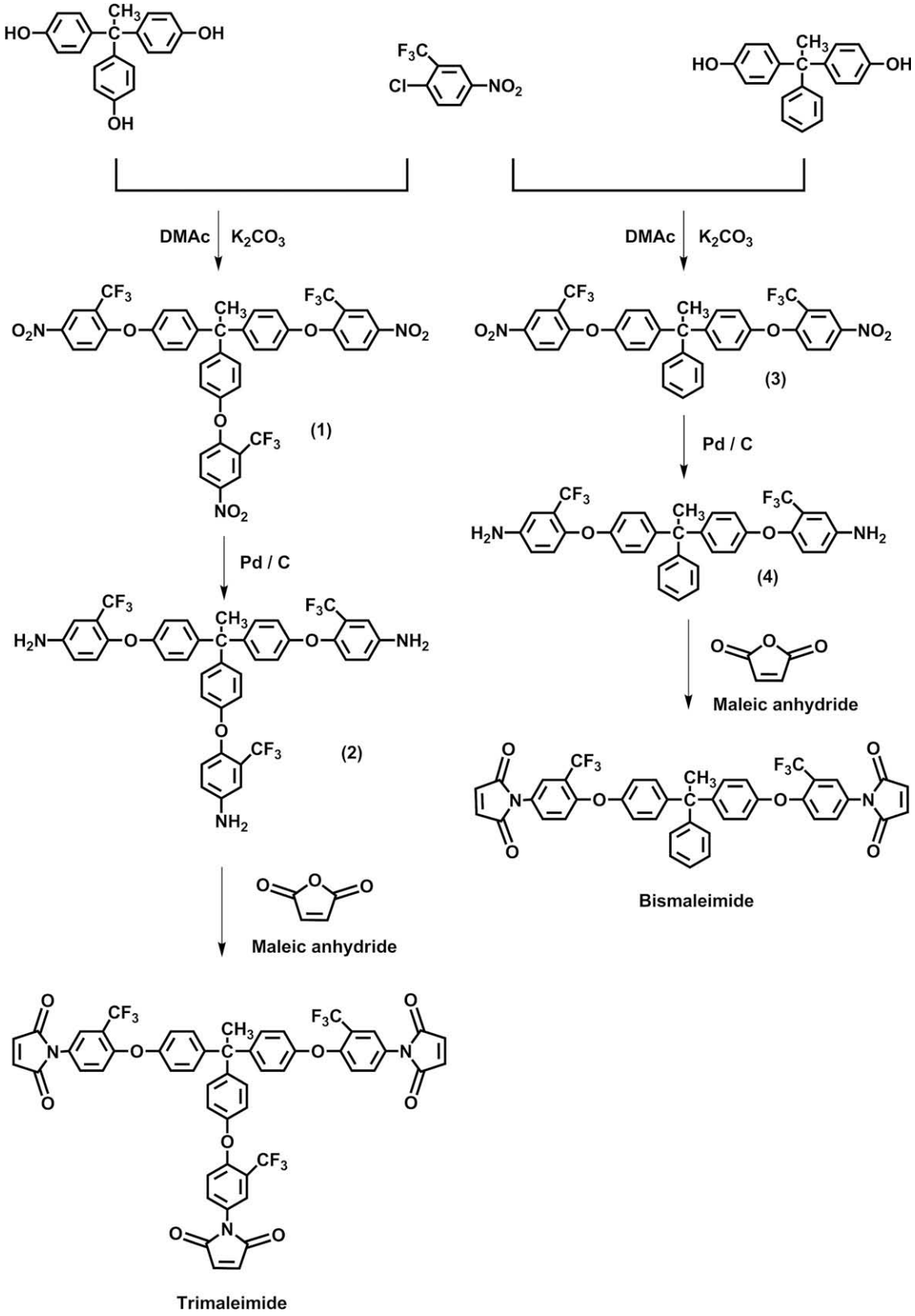

Fig. 1. Synthesis of the trimaleimide and bismaleimide monomers.

remove the solvent. The obtained mixture was poured into water to wash redundant hydrazine monohydrate. The precipitate is cream-colored crystals after drying under vacuum at 50 °C. Yield: 70.4%.

$C_{34}H_{26}F_6N_2O_2$ (608.19): Calcd. C 67.10%, H 4.31%, N 4.60%; Found C 66.57%, H 4.57%, N 4.90%.

^{1}H NMR (DMSO-d_6): $\delta_{ppm} = 6.71–7.40$ (m, Ar-H), 5.42 (s, $-NH_2$) and 2.09 (s, $-CH_3$).

IR (KBr): 1046 and 1261 cm^{-1} (–C═O), 3383 and 3467 cm^{-1} ($–NH_2$).

2.6. Synthesis of 1,1-bis [4-(4-maleimide-2-trifluoromethylphenoxy)-phenyl]-1-phenylethane (bismaleimide; Fig. 1)

Compound **4** (1.22 g, 2 mmol) was first dissolved in 10 cm^3 DMAc in a 100 cm^3 flask. After the mixture was completely dissolved, maleic anhydride (0.78 g, 8 mmol) was added. The solution was stirred at room temperature for 12 h and then acetic anhydride (1.12 g, 1.1 mmol) and sodium acetate (1.65 g, 2 mmol) were added to the solution at 60 °C. The solution was stirred for another 0.8 h. The product was purified by re-precipitations into water, and dried under vacuum. Yield: 71.8%.

$C_{42}H_{26}F_6N_2O_6$ (768.17): Calcd. C 65.63%, H 3.41%, N 3.64%; Found C 65.59%, H 3.81%, N 3.61%.

^{1}H NMR ($CDCl_3$): $\delta_{ppm} = 2.14$ (3H, s, $–CH_3$), 6.81 (4H, s, (maleimide) CH═CH), 6.96–7.30 (15H, m, Ar–H & (Ar–CF_3)–H), 7.39 (2H, d, (Ar–CF_3)–H), 7.60 (2H, s, (Ar–CF_3)–H).

IR (KBr): 828 and 3098 cm^{-1} (═C–H of maleimide), 1320 cm^{-1} (–C–N), 1720 cm^{-1} (–C═O).

FAB MS: m/z 768 (M^+).

2.7. Synthesis of 2,4-diamino-4′-(4-nitrophenyl-diazenyl) azobenzene (DNDA; Fig. 2) [38,39]

DO_3 (0.24 g, 1 mmol), $NaNO_2$ (0.07 g, 1 mmol), 15 cm^3 of ice water, and 15 cm^3 of dimethyl sulfoxide (DMSO) were mixed with 5.5 cm^3 of concentrated hydrochloric acid. The mixture was stirred for 0.5 h in an ice bath and then slowly poured into a solution containing 1.5 mmol (0.16 g) of *m*-phenylenediamine and 36 cm^3 of methanol/water co-solvent (2/1 in volume ratio). The mixture was stirred vigorously for 1 h and then neutralized with sodium acetate to pH 5–6. After further stirring for 0.5 h, the mixture was filtered. Subsequently, the precipitate was dried. Yield: 88%.

$C_{18}H_{15}N_7O_2$ (361.13): Calcd. C 59.83%, H 4.18%, N 27.13%; Found C 59.35%, H 4.54%, N 26.48%.

^{1}H NMR (DMSO-d_6): $\delta_{ppm} = 5.86–8.44$ (m, Ar-H), 6.32 (s, $–NH_2$).

FTIR (KBr): 3480–3392 cm^{-1} ($–NH_2$), 1514–1342 cm^{-1} ($–NO_2$), 1730 cm^{-1} (–N═N).

2.8. Synthesis of NLO polymers (Fig. 3)

2.8.1. Linear polymers

Compositions for the NLO linear and hyperbranched polymers are shown in Table 1. The linear polymers were synthesized via Michael addition reaction. For the linear polymer, LDAC11 (Table 1), bis(4-aminophenyl(4-(4-nitrophenyl)-diazenyl)-phenyl)amine (DAC) was first synthesized according to the literature [40]. Bismaleimide (0.92 g, 1.2 mmol) was dissolved in 25 cm^3 of DMAc in a 100 cm^3 flask with stirring. After complete dissolution, DAC (0.51 g, 1.2 mmol) was added to the solution using *p*-toluenesulfonic acid (*p*-TSA) (1.02 g) as catalyst. The mixture was stirred and heated to 120 °C, and further remained under dry nitrogen atmosphere for 100 h. The product was purified by re-precipitations into methanol, and dried in vacuum at 70 °C for 12 h.

For the other linear polymer, LDNDA11 (Table 1), bismaleimide (0.92 g, 1.2 mmol) was first dissolved in 25 cm^3 of DMAc in a 100 cm^3 flask. After complete dissolution, DNDA (0.43 g, 1.2 mmol) was added to the solution using *p*-TSA (1.02 g) as catalyst. The mixture was stirred and heated to 120 °C, and further remained under dry nitrogen atmosphere for 100 h. The product was purified by re-precipitations into methanol, and dried in vacuum at 70 °C for 12 h.

2.8.2. Hyperbranched polymers

Hyperbranched polymers, HBDAC11, HBDAC23 and HBDAC12 (Table 1) were synthesized by reacting the difunctional azobenzene dye DAC with trimaleimide at different molecular ratios. The trimaleimide was dissolved in 20 cm^3 of DMAc. After complete dissolution, the difunctional compound (DAC) was added to the solution. These mixtures were heated to 120 °C and reacted under a dry nitrogen atmosphere for 100 h, using *p*-TSA (1.02 g) as catalyst. The product was separated by re-precipitations into methanol, purified, and dried in vacuum at 70 °C for 12 h.

Hyperbranched polymers, HBDNDA11, HBDNDA23 and HBDNDA12 (Table 1) were synthesized by reacting the difunctional azobenzene dye DNDA with trimaleimide at different molecular ratios. The trimaleimide was dissolved in 20 cm^3 of DMAc. After complete dissolution, the difunctional compound (DNDA) was added to the solution. These mixtures were heated to 120 °C and reacted under a dry nitrogen atmosphere for 72 h, using *p*-TSA (1.02 g) as catalyst. The product was purified by re-precipitations into methanol, and dried in vacuum at 70 °C for 12 h.

2.9. Thin film preparation

These polymers were respectively dissolved in DMF. The polymer solution was stirred at room temperature for 3 h, and filtered through a 1-μm syringe filter. Thin films were prepared by spin-coating the filtered polymer solution onto indium tin oxide (ITO)

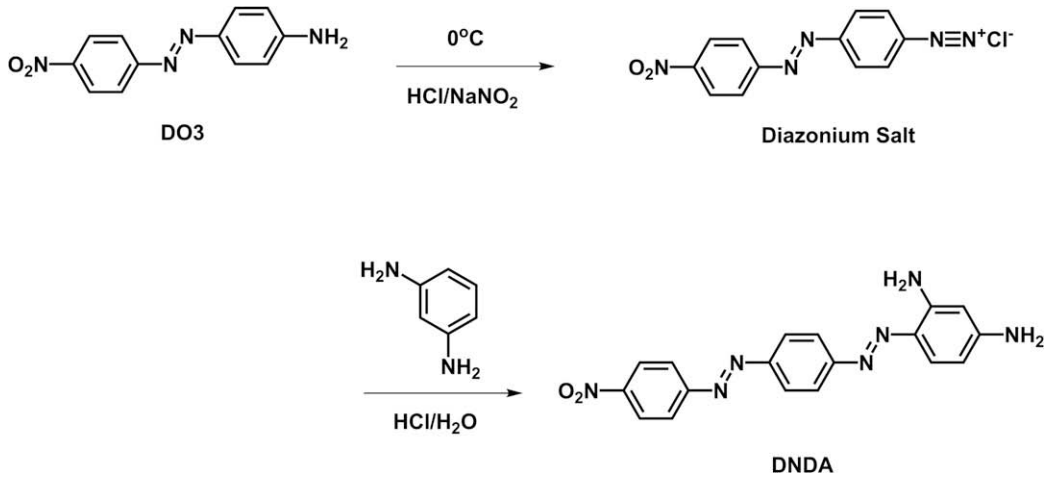

Fig. 2. Synthesis of the azobenzene dye, DNDA.

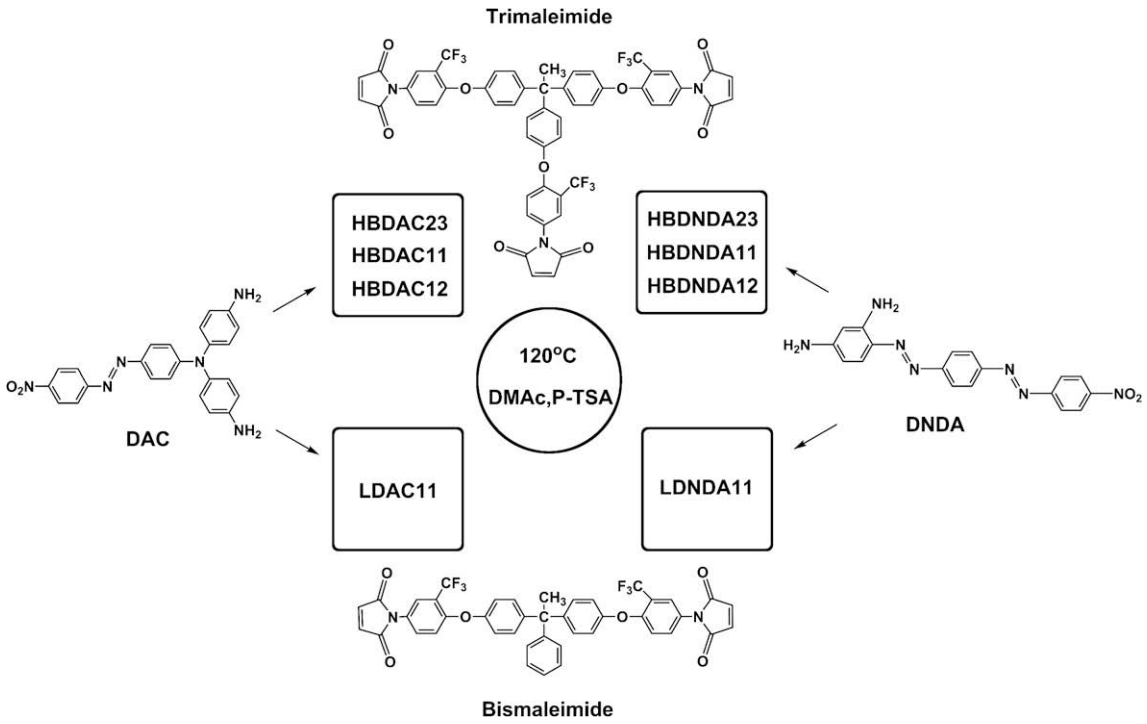

Fig. 3. Synthesis of the polyaspartimides.

glass substrates. Prior to the poling process, these thin films were dried in vacuum at 70 °C for 24 h.

2.10. Poling process and electro-optical (EO) coefficient (r_{33}) measurement

Poling processes for the polymer films were carried out using an *in situ* contact poling technique [41]. The poling voltage was maintained at 100 V and the temperature was kept at approximately 10 °C lower than the T_g of the sample for a certain period of time. The non-centrosymmetric alignment of the NLO dyes was achieved during this period. Upon saturation of the r_{33} signal intensity, the sample was then cooled down to room temperature in the presence of the poling field at which point the poling field was terminated. The thickness and refractive indices were measured at 830 nm by a Spectroscopic Ellipsometer (J.A. Wollam Co, Inc. MW2000). EO coefficients of the poled samples were measured at 830 nm using the simple reflection technique [42].

2.11. Optical loss measurement [43–45]

For the optical loss measurement, a laser beam (830 nm) passed through a linear polarizer and a polarizing beam splitter. Subsequently, the TE polarized light was focused onto a prism coupler that was mounted on a rotation stage. The scattered light was imaged with an infrared-sensitive charge-injection-device camera system. A statistical linear fit of the data to the logarithm of the scattered light intensity versus the distance propagated down the waveguide yielded a waveguide loss as a slope.

3. Results and discussion

A series of new NLO hyperbranched polyaspartimides have been synthesized via Michael addition reaction between trimaleimide and two respective azobenzene dyes, DAC and DNDA. In comparison with the preparation of dendrimers via a convergent or divergent route, the one-pot synthesis of hyperbranched polymers is drastically simplified.

The azobenzene dye, DNDA was prepared by an azo coupling reaction. Maleimide-containing monomers for synthesizing polyaspartimides were prepared according to the routes as shown in Fig. 1, [46]. All of the monomers were characterized with FTIR, ^{1}H NMR and EA. According to a previous investigation [28], the polymerization is usually achieved with *o*-cresol as the solvent. However, the *o*-cresol solvent is highly toxic. Hence, another solvent, *N*,*N*-dimethylacetamide (DMAc), was used instead of *o*-cresol in this research [27].

FTIR was utilized to monitor the reaction progress. For example, the hyperbranched polymer, HBDNDA23 was obtained via the reaction between DNDA (A_2 type monomer) and trimaleimide (B_3 type monomer). The azobenzene dye, DNDA with two amine groups is capable of performing Michael addition reaction toward trimaleimide at higher temperatures, using *p*-TSA as the catalyst. FTIR spectra of the HBDNDA23 sample are shown in Fig. 4. The spectra exhibited two characteristic absorption bands at 1720 cm^{-1} and 1780 cm^{-1} due to the C═O stretching from the imide ring, and

Table 1
Compositions (molar ratios) and abbreviated names for the NLO-active linear and hyperbranched polymers.

Linear polymer			
Dimaleimide	DAC	DNDA	Abbreviated names for samples
1	1	0	LDAC11
1	0	1	LDNDA11
Hyperbranched polymer			
Trimaleimide	DAC	DNDA	Abbreviated names for samples
1	1	0	HBDAC11
2	3	0	HBDAC23
1	2	0	HBDAC12
1	0	1	HBDNDA11
2	0	3	HBDNDA23
1	0	2	HBDNDA12

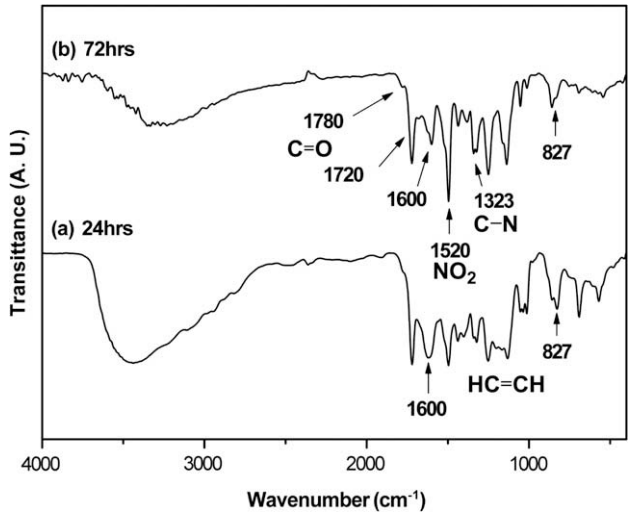

Fig. 4. FTIR spectra of HBDNDA23 (a) reaction for 24 h and (b) reaction for 72 h.

a characteristic absorption band at 1320 cm^{-1} due to the imide C–N stretching. These results support the formation of the imide groups. When the reaction between maleimide and amine groups was completed, the absorption bands from the CH═CH group of maleimide (827 cm^{-1}) became less obvious. Moreover, the characteristic absorption bands of the asymmetrical and symmetrical stretching of the nitro groups were also evident at approximately 1500 and 1342 cm^{-1}, respectively, clearly indicating the presence of the NLO dye in the polymer. Similar FTIR spectra were also observed for the remaining samples.

The solubility of the polyaspartimides in various solvents is summarized in Table 2. All of the polymers are soluble at room temperature in polar aprotic solvents such as DMF, DMAc and DMSO. Except HBDNDA23 and HBDNDA12, most of them are soluble in the common organic solvent, THF. Moreover, these polymers are partially soluble in acetone and chloroform. The DAC-containing polymer systems consisting of azobenzene dyes with a shorter conjugate length would exhibit better solubility in organic solvents. Because of their excellent solubility, the molecular weights of these polymers were determined by GPC using DMF as eluent (Table 3). The weight average molecular weight of the polymers was in the range of 6000–11,500. For the same reaction time, the molecular weights of the hyperbranched polymers are higher than that of the linear polymer. Normally, the molecular weights of the hyperbranched polymers might be higher than the result obtained by GPC measurements because linear polystyrene was used as a standard in this measurement [16,37]. This indicates that the hyperbranched polymers exhibit a higher degree of polymerization than the linear polymer.

Table 2
Solubility properties of the polymers.

Samples	Solvents[a]						
	DMAc	DMF	DMSO	THF	Acetone	$CHCl_3$	MeOH
LDAC11	++[b]	++	++	++	++	+−	−−[b]
HBDAC23	++	++	++	++	+−	+−	−−
HBDAC11	++	++	++	++	+−	+−	−−
HBDAC12	++	++	++	++	+−	+−	−−
LDNDA11	++	++	++	++	+−	+−	−−
HBDNDA23	++	++	++	+−[b]	+−	+−	−−
HBDNDA11	++	++	++	++	+−	+−	−−
HBDNDA12	++	++	++	+−	+−	+−	−−

[a] THF: tetrahydrofuran, DMAc: dimethylacetamide, DMSO: dimethyl sulfoxide, DMF: *N*,*N*-dimethyl formamide, $CHCl_3$: chloroform, MeOH: methanol.
[b] (++): soluble at room temperature; (+−): partially soluble; (−−): insoluble.

Table 3
Thermal properties and molecular weights of the polymers.

Samples	T_d[a] (°C)	T_g (°C)	M_n[b]	M_w[b]
LDAC11	252.8	116.0	4479	6054
HBDAC11	268.5	172.1	4727	8727
HBDAC23	279.7	171.1	4955	8456
HBDAC12	268.5	169.4	4226	7773
LDNDA11	244.4	112.7	6679	7392
HBDNDA11	257.3	144.6	7770	10185
HBDNDA23	301.8	132.7	9303	11830
HBDNDA12	235.0	119.8	7896	11549

[a] T_d was read at the temperature corresponding to 5% wt loss.
[b] Determined by GPC in DMF with polystyrene standards.

Thermal properties of the linear and hyperbranched polymers were measured with DSC and TGA (Table 3). The T_gs of the HBDNDA system are in the range between 119.8 and 144.6 °C, whereas the T_g of LDNDA11 is observed at 112.7 °C. DSC thermograms of LDAC11 and HBDAC systems are shown in Fig. 5. For the HBDAC system, T_gs ranging from 169.4 to 172.1 °C are obtained, whereas the T_g of LDAC11 is located at 116.0 °C. For the above-mentioned two systems, the T_g of linear polymer is lower than those of the hyperbranched polymers. This might be due to the fact that the molecular weights of the hyperbranched polymers are higher than that of the linear polymer. In addition, the presence of side chain azobenzene dyes would prevent tight packing among the polymer chains, which leads to a decrease in intermolecular interactions. On the other hand, the hyperbranched polymer having a highly branched and globular structure would enhance the intermolecular interactions [47]. Moreover, it is important to note that the T_g decreased with increasing content of azobenzene dye in the hyperbranched polymers. This is because the composition of end groups in the hyperbranched polymers can exert a significant effect on intramolecular and intermolecular interactions, which would manifest in thermal properties [48–50]. Moreover, the azobenzene dye is less rigid than trimaleimide. In HBDNDA system, the HBDNDA12 polymer with the highest dye content in the terminal groups would certainly exhibit the lowest T_g among the hyperbranched polymers. Furthermore, the T_gs of HBDAC system are higher than those of HBDNDA system while their molar ratios of maleimide to dye are the same. This might be due to the DNDA dye possessing a longer conjugate length than the DAC dye. The longer conjugate length structure with higher rigidity would possibly hinder the close packing of polymer chains. This results in a decrease in intermolecular interactions [51]. According to the

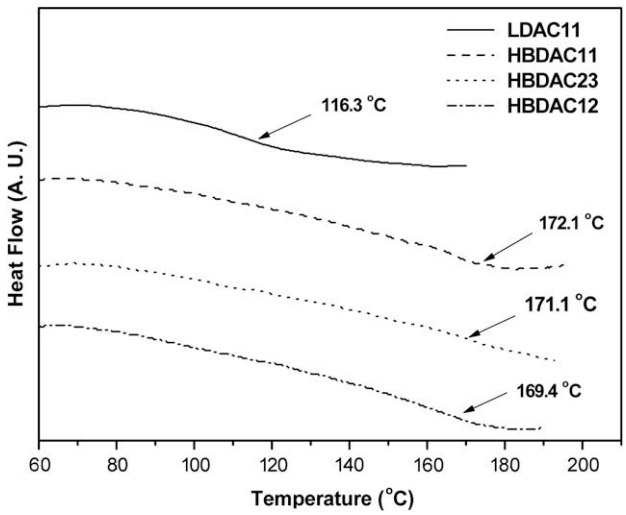

Fig. 5. DSC thermograms of the LDAC11 and HBDAC systems.

literature [52,53], the T_g of a polarly functionalized cascade branched polymer mainly depends on the interactions of the end groups. In contrast to the linear polymers, the end group influence on the T_g does not vanish with increasing molecular weight for the hyperbranched polymers. This is because the number of end groups is proportional to the degree of polymerization. Hence, the T_gs of the HBDAC system are still higher than those of the HBDNDA system with the same molar ratios, despite that the molecular weights of the DAC system are lower than those of the DNDA system.

Absorption characteristics of polymer films were investigated by UV–vis spectrophotometry. For the DNDA-containing system, the absorption maximum was located around 536 nm, whereas the cut-off wavelength was 815 nm. The DAC-containing system exhibited an absorption maximum and cut-off wavelength at 507 and 800 nm, respectively. Because of the presence of a longer π-conjugated length, a red shift was obtained for the DNDA-containing system as compared to the DAC-containing system. In addition, the EO coefficients were measured at 830 nm in order to circumvent the absorption range.

Unlike linear polymers, hyperbranched polymers possess globular structures [54]. Moreover, their three-dimensional structures help to reduce the aggregation of the conjugated polymer chains and to improve their luminescent efficiency [55]. It is thus expected that hyperbranched polymers would exhibit unique optical properties different from those of the corresponding linear polymers. To generate stable oriented dipoles and large EO coefficients, the NLO-active polymers should be aligned and annealed under an electric field. By spin-coating the linear and hyperbranched polymer solutions onto ITO glasses, optical quality films were obtained. Optical properties of these NLO materials are shown in Table 4. Thicknesses of the polymer films ranged from 1.6 to 2.3 μm, whereas refractive indices ranged from 1.57 to 1.63 (830 nm). The dye contents were determined by UV–vis investigations [56,57]. EO coefficients resulted from the *in situ* poling process ranged from 6.5 to 14.7 pm/V (measured at 830 nm). The r_{33} values of all hyperbranched polymers are proportional to their dye contents. This implies that aggregation of NLO dyes did not take place. It is important to note that the aggregation problem is often found in linear polymer systems [58]. With similar dye contents, the poled films of HBDAC23 and HBDAC12 exhibited r_{33} values of 11.3 and 13.4 pm/V, respectively, which are two times larger than that of LDAC11, indicating a significant improvement in poling efficiency. More importantly, the r_{33} value of the hyperbranched polymer HBDAC11 is larger than that of the linear polymer LDAC11 even though the linear polymer LDAC11 possesses a larger dye content than HBDAC11. This is possibly due to the presence of a spherical shape and site isolation effect in the hyperbranched structure. Similar results are also observed for the DNDA-containing samples. Furthermore, with similar dye contents, the r_{33} value of the DNDA-containing system is larger than that of the DAC-containing system. This is due to the fact that the conjugated length of DNDA azobenzene dye is longer than that of DAC azobenzene dye.

Table 4
Optical properties of the DAC- and DNDA-based NLO polymers.

Samples	Dye content (%)	Thickness film (μm)	Refraction indices at 830 nm	r_{33} (pm/V) at 830 nm	Optical loss (dB/cm) at 830 nm
LDAC11	21.6	1.8	1.61	6.5	4.3
HBDAC11	19.2	1.7	1.59	9.8	3.3
HBDAC23	22.1	2.3	1.60	11.3	3.6
HBDAC12	25.1	2.0	1.63	13.4	4.5
LDNDA11	18.6	1.6	1.58	7.1	4.5
HBDNDA11	12.4	2.1	1.57	8.4	2.5
HBDNDA23	18.5	1.9	1.58	13.9	3.1
HBDNDA12	21.0	1.7	1.59	14.7	3.9

In general, the EO coefficient of the NLO polymer remains stable at low temperatures, but decays significantly at a specific temperature. This specific temperature is defined as the effective relaxation temperature [59]. This value allows quick evaluation of the temporal and thermal stability of the materials. In the investigation of dynamic thermal stability, only the samples with better thermal stability (DAC system) were measured at 830 nm. Dynamic thermal stability of the NLO activities of the linear polymer (LDAC11; dye content: 21.6%) and hyperbranched polymer (HBDAC23; dye content: 22.1%) with similar dye contents was investigated by depoling experiments. Fig. 6 shows the dynamic thermal stability of the poled LDAC11 and HBDAC23 samples. Apparently, the HBDAC23 example exhibits a higher effective relaxation temperature as compared to the linear polymer LDAC11. As mentioned previously, the hyperbranched polymer possessing highly branched and globular structure would construct a more compact structure than the corresponding linear one. Therefore, the hyperbranched polymer systems are somewhat more effective to restrict the mobility of the aligned NLO dyes as compared to the linear polymers.

In the investigation of the temporal stability of the EO coefficient, only the samples with better thermal stability (DAC system) were measured at 830 nm. Fig. 7 shows the temporal stability of the EO coefficient for the poled DAC-containing system at 80 °C for 200 h. At the beginning of thermal treatment, a fast decay of the EO coefficients was perceived. This phenomenon might result from the recovery of bond angle and bond length of the oriented azobenzene dyes [60]. After being subjected to thermal treatment at 80 °C for 200 h, a reduction of less than 20% in the EO coefficient ($r_{33}(t)/r_{33}(t_0)$) is observed for hyperbranched polymers due to the presence of high T_gs. On the other hand, a reduction of more than 50% in the EO coefficient is observed for the linear polymer, LDAC11. A much better temporal stability is obtained for the hyperbranched polymers. This indicates that the T_g is the sole deciding factor responsible for the temporal stability in this work.

In the investigation of optical loss, the transmission losses of the optical waveguides, only the TE guide modes at 830 nm are considered. As shown in Table 4, the optical losses of those polymers are in the range 2.5–4.5 dB/cm. Conspicuously, the optical loss is increased with increasing dye content, which is consistent with results reported by other researchers [61]. Furthermore, the HBDNDA11 sample exhibits the lowest optical loss than the rest of samples in the DNDA-containing series. Similar results are also observed for HBDAC11 in the DAC-containing system. This is possibly due to the fact that a relatively lower dye content in both

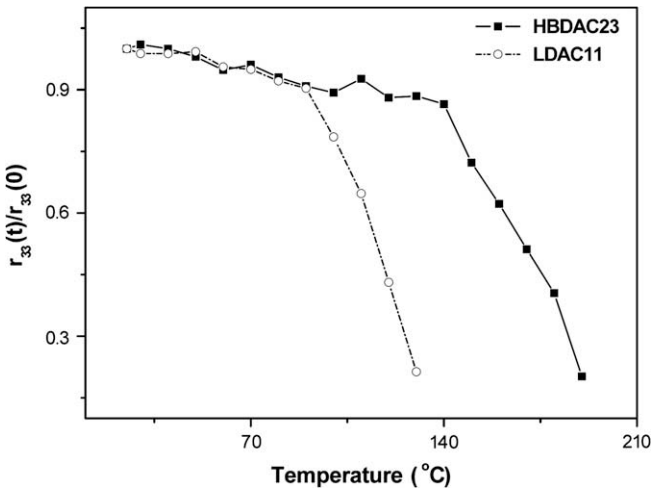

Fig. 6. Temperature dependence of the dipole re-orientational dynamics of the poled LDAC11 and HBDAC23 samples.

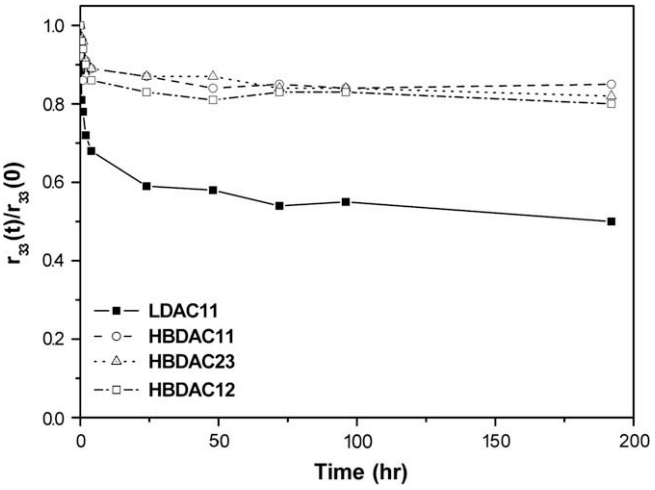

Fig. 7. Temporal stability of EO coefficients for the poled LDAC11 and HBDAC systems at 80 °C.

HBDNDA11 and HBDAC11 and the introduction of fluorine-containing functionalities (trimaleimide) result in reducing the density of C–H, O–H and N–H bonds in the intrinsic structures. This plays a key role in lowering the optical loss of these materials. In addition, lower optical losses are obtained for the hyperbranched polymers when compared with the linear polymer. The uniform void-rich topological structure of hyperbranched polymers might possibly help to minimize the optical losses [18,19]. Further optimization of materials and processing conditions is expected to minimize the optical losses of the polymers [44,45,62]. In this particular area, direct introduction of fluorine atoms to azobenzene dyes and polyaspartimides structures seems to provide lower optical losses [63].

4. Conclusion

Through Michael addition reaction, two thermally stable NLO hyperbranched systems consisting of azobenzene dyes were successfully synthesized. All of the obtained polymers are soluble in DMF, DMAc and DMSO. By incorporating the polyaspartimide structure into the NLO-active hyperbranched polymers, the thermal stability was greatly enhanced. Using *in situ* contact poling, r_{33} coefficients of 6.5–14.7 pm/V and temporal stability at 80 °C were obtained. In addition, all the hyperbranched polymers exhibit better NLO properties than their corresponding linear analogues, due to the presence of a spherical shape and site isolation effect. Waveguide properties are also achieved for all of the NLO polymers.

Acknowledgement

Financial support from National Science Council, Taiwan is gratefully acknowledged. This work is also supported in part by the Ministry of Education, Taiwan under ATU plan. The authors would like to thank Prof. E. Conte of West Kentucky University, USA for technical editing.

References

[1] Haller M, Luo JD, Li HX, Kim TD, Liao Y, Robinson B, et al. A novel lattice-hardening process to achieve highly efficient and thermally stable nonlinear optical polymers. Macromolecules 2004;37(3):688–90.
[2] Chen L, Qian G, Gui Y, Jin X, Wang Z, Wang MJ. Hybrid materials covalently incorporated with isophorone-based dyes through sol–gel process for nonlinear optical applications. Journal of Physical Chemistry B 2006;110(39):19176–82.
[3] Zhang C, Dalton LR, Oh MC, Zhang H, Steier W. Low $V\pi$ electrooptic modulators from CLD-1: chromophore design and synthesis, material processing, and characterization. Chemistry of Materials 2001;13(9):3043–50.
[4] Verbiest T, Houbrechts S, Kauranen M, Clays K, Persoons A. Second-order nonlinear optical materials: recent advances in chromophore design. Journal of Materials Chemistry 1997;7(11):2175–89.
[5] Zhang CZ, Lu C, Zhu J, Lu GY, Wang X, Shi ZW, et al. The second-order nonlinear optical materials with combined nonconjugated D-π-A units. Chemistry of Materials 2006;18(26):6091–3.
[6] Dalton LR, Harper A, Ren A, Wang W, Todorova G, Chen J, et al. Polymeric electro-optic modulators: from chromophore design to integration with semiconductor very large scale integration electronics and silica fiber optics. Industrial and Engineering Chemistry Research 1999;38(1):8–33.
[7] Ma H, Chen B, Sassa T, Dalton LR, Jen AKY. Highly efficient and thermally stable nonlinear optical dendrimer for electrooptics. Journal of the American Chemical Society 2001;123(5):986–7.
[8] Ma H, Jen AKY. Functional dendrimers for nonlinear optics. Advanced Materials 2001;13(15):1201–5.
[9] Do JY, Park SK, Ju JJ, Park S, Lee MH. Electro-optic materials: hyperbranched chromophores attached linear polyimide and dendritic polyesters. Polymers for Advanced Technologies 2005;16(2–3):221–6.
[10] Robinson BH, Dalton LR. Monte carlo statistical mechanical simulations of the competition of intermolecular electrostatic and poling-field interactions in defining macroscopic electro-optic activity for organic chromophore/polymer materials. Journal of Physical Chemistry A 2000;104(20):4785–95.
[11] Sullivan PA, Akelaitis AJP, Lee SK, McGrew G, Lee SK, Choi DH, et al. Novel dendritic chromophores for electro-optics: influence of binding mode and attachment flexibility on electro-optic behavior. Chemistry of Materials 2006;18(2):344–51.
[12] Zhu Z, Li Z, Tan Y, Li Z, Li Q, Zeng Q, et al. New hyperbranched polymers containing second-order nonlinear optical chromophores: synthesis and nonlinear optical characterization. Polymer 2006;47(23):7881–8.
[13] Ma H, Wu J, Herguth P, Chen B, Jen AKY. A novel class of high-performance perfluorocyclobutane-containing polymers for second-order nonlinear optics. Chemistry of Materials 2000;12(5):1187–9.
[14] Do JY, Ju JJ. Polyester dendrimers carrying NLO chromophores: synthesis and optical characterization. Macromolecular Chemistry and Physics 2005;206(13):1326–31.
[15] Fréchet JMJ, Henmi M, Gitsov I, Aoshima S, Leduc MR, Grubbs RB. Self-condensing vinyl polymerization: an approach to dendritic materials. Science 1995;269:1080–3.
[16] Li Z, Qin A, Lam JWY, Dong Y, Dong Y, Ye C, et al. Facile synthesis, large optical nonlinearity, and excellent thermal stability of hyperbranched poly (aryleneethynylene)s containing azobenzene chromophores. Macromolecules 2006;39(4):1436–42.
[17] Hecht S, Fréchet JMJ. Dendritic encapsulation of function. Angewandte Chemie International Edition 2001;40(1):74–91.
[18] Ma H, Liu S, Luo J, Suresh S, Liu L, Kang SH, et al. Highly efficient and thermally stable electro-optical dendrimers for photonics. Advanced Functional Materials 2002;12(9):565–74.
[19] Zhou Z, Yan D. Distribution function of hyperbranched polymers formed by AB_2 type polycondensation with substitution effect. Polymer 2006;47(4):1473–9.
[20] Chang HL, Chao TY, Yang CC, Dai SA, Jeng RJ. Second-order nonlinear optical hyperbranched polymers via facile ring-opening addition reaction of azetidine-2,4-dione. European Polymer Journal 2007;43(9):3988–96.
[21] Xie J, Deng X, Cao Z, Shen Q, Zhang W, Shi W. Synthesis and second-order nonlinear optical properties of hyperbranched polymers containing pendant azobenzene chromophores. Polymer 2007;48(20):5988–93.
[22] Xie J, Hu L, Shi W, Deng X, Cao Z, Shen Q. Synthesis and nonlinear optical properties of hyperbranched polytriazole containing second-order nonlinear optical chromophores. Journal of Polymer Science Part B: Polymer Physics 2008;46(12):1140–8.
[23] Jeng RJ, Chang CC, Chen CP, Chen CT, Su WC. Thermally stable crosslinked NLO materials based on maleimides. Polymer 2003;44(1):143–55.
[24] Jeng RJ, Hung WY, Chen CP, Hsiue GH. Organic/inorganic NLO materials based on reactive polyimides and a bulky alkoxysilane dye via sol/gel process. Polymers for Advanced Technologies 2003;14(1):66–75.
[25] Lu J, Yin J. Synthesis and characterization of photocrosslinkable, side-chain, second-order nonlinear optical poly(ester imide)s with great film-forming ability and long-term dipole orientation stability. Journal of Polymer Science Part A: Polymer Chemistry 2003;41(2):303–12.
[26] Bell VL, Young PR. Isomeric bismaleimides and polyaspartimides. Journal of Polymer Science Part A: Polymer Chemistry 1986;24(10):2647–55.
[27] Wu CS, Liu YL, Chiu YS. Synthesis and characterization of new organosoluble polyaspartimides containing phosphorus. Polymer 2002;43(6):1773–9.
[28] Liaw DJ, Liaw BY, Chen JJ. Synthesis and characterization of new soluble polyaspartimides derived from bis(3-ethyl-5-methyl-4-maleimidophenyl)-methane and various diamines. Polymer 2001;42(3):867–72.
[29] Tungare AV, Martin GC. Analysis of the curing behavior of bismaleimide resins. Journal of Applied Polymer Science 1992;46(7):1125–35.
[30] Curliss DB, Cowans BA, Caruthers JM. Cure reaction pathways of bismaleimide polymers: a solid-state ^{15}N NMR investigation. Macromolecules 1998;31(20):6776–82.
[31] Huang F, Gibson HW. Formation of a supramolecular hyperbranched polymer from self-organization of an AB_2 monomer containing a crown ether and two paraquat moieties. Journal of the American Chemical Society 2004;126(45):14738–9.

[32] Baek JB, Harris FW. Fluorine- and hydroxyl-terminated hyperbranched poly(phenylquinoxalines) (PPQs) from copolymerization of self-polymerizable AB and AB_2, BA, and BA_2 monomers. Macromolecules 2005;38(4):1131–40.
[33] Che P, He Y, Wang X. Hyperbranched azo-polymers synthesized by azo-coupling reaction of an AB_2 monomer and postpolymerization modification. Macromolecules 2005;38(21):8657–63.
[34] Baek JB, Harris FW. Hyperbranched polyphenylquinoxalines from self-polymerizable AB_2 and A_2B monomers. Macromolecules 2005;38(2):297–306.
[35] Hao J, Jikei M, Kakimoto MA. Preparation of hyperbranched aromatic polyimides via $A_2 + B_3$ approach. Macromolecules 2002;35(14):5372–81.
[36] Chen H, Yin J. Synthesis and characterization of negative-type photosensitive hyperbranched polyimides with excellent organosolubility from an $A_2 + B_3$ monomer system. Journal of Polymer Science Part A: Polymer Chemistry 2004;42(7):1735–44.
[37] Liu YL, Tsai SH, Wu CS, Jeng RJ. Preparation and characterization of hyperbranched polyaspartimides from bismaleimides and triamines. Journal of Polymer Science Part A: Polymer Chemistry 2004;42(23):5921–8.
[38] Saadeh H, Gharavi A, Tu D, Yu LP. Polyimides with a diazo chromophore exhibiting high thermal stability and large electrooptic coefficients. Macromolecules 1997;30(18):5403–7.
[39] Balcerzak ES, Grabiec E, Sek D, Miniewicz A. New azobenzene chromophores as monomers for synthesis of polyesters. Polymer Journal 2003;35:851–8.
[40] Mandal BK, Jeng RJ, Kumar J, Tripathy SK. New photocrosslinkable polymers for second-order nonlinear optical processes. Macromolecular Rapid Communications 1991;12(11):607–12.
[41] Chang HL, Lin HL, Wang YC, Dai SA, Su WC, Jeng RJ. Thermally stable NLO poly(amide-imide)s via sequential self-repetitive reaction. Polymer 2007;48(7):2046–55.
[42] Teng CC, Man HT. Simple reflection technique for measuring the electro-optic coefficient of poled polymers. Applied Physics Letters 1990;56(18):1734–7.
[43] Shi W, Fang CS, Pan QW, Gu QT, Xu D, Wei HZ, et al. Measurement of the optical transmission modes and losses of the poled guest–host polymer NAEC/PEK-c planar waveguides. Optics and Lasers in Engineering 2000;33(1):21–8.
[44] Shi W, Fang CS, Sui Y, Yin J, Pan QW, Gu QT, et al. Poling optimization and optical loss measurement of the polyetherketone polymer films. Solid State Communications 2000;116(2):67–71.
[45] Shi W, Fang CS, Sui Y, Yin J, Pan QW, Gu QT, et al. Thermal stability and transmission losses of the poled polyimide side-chain thin films. Optics Communications 2000;183(1–4):299–306.
[46] Liu YL, Jeng RJ, Chiu YS. Triphenylphosphine oxide-based bismaleimide and poly(bismaleimide): synthesis, characterization, and properties. Journal of Polymer Science Part A: Polymer Chemistry 2001;39(10):1716–25.
[47] Borah J, Mahapatra SS, Saikia D, Karak N. Physical, thermal, dielectric and chemical properties of a hyperbranched polyether and its linear analog. Polymer Degradation and Stability 2006;91(12):2911–6.
[48] Vogtle F, Gestermann S, Hesse R, Schwierz H, Windisch BF. Functional dendrimers. Progress in Polymer Science 2000;25(7):987–1041.
[49] Voit B. New developments in hyperbranched polymers. Journal of Polymer Science Part A: Polymer Chemistry 2000;38(14):2505–25.
[50] Sendijarevic I, McHugh AJ, Markoski LJ, Moore JS. Eliminating variations in elemental composition in studies on the physical properties of linear to hyperbranched etherimide copolymers. Macromolecules 2001;34(25):8811–3.
[51] Sui Y, Liu YG, Yin J, Gao J, Zhu ZK, Huang DY, et al. Study on side-chain second-order nonlinear optical polyimides based on novel chromophore-containing diamine. 1. Synthesis and characterization. Journal of Polymer Science Part A: Polymer Chemistry 1999;37(23):4330–6.
[52] Stutz H. The glass temperature of dendritic polymers. Journal of Polymer Science Part B: Polymer Physics 1995;33(3):333–40.
[53] Sunder A, Bauer T, Mülhaupt R, Frey H. Synthesis and thermal behavior of esterified aliphatic hyperbranched polyether polyols. Macromolecules 2000;33(4):1330–7.
[54] Kwak G, Masuda T. Synthesis, characterization and optical properties of a novel si-containing σ–π-conjugated hyperbranched polymer. Macromolecular Rapid Communications 2002;23(1):68–72.
[55] Sun M, Bo Z. Tuning the optical properties of hyperbranched polymers through the modification of the end groups. Journal of Polymer Science Part A: Polymer Chemistry 2007;45(1):111–24.
[56] Song N, Men L, Gao JP, Bai Y, Beaudin AMR, Yu G, et al. Cross-linkable zwitterionic polyimides with high electrooptic coefficients at telecommunication wavelengths. Chemistry of Materials 2004;16(19):3708–13.
[57] Luo JD, Haller M, Li HX, Tang HZ, Jen AKY. A side-chain dendronized nonlinear optical polyimide with large and thermally stable electrooptic activity. Macromolecules 2004;37(2):248–50.
[58] Bai YW, Song NH, Gao JP, Sun X, Wang XM, Yu GM, et al. A new approach to highly electrooptically active materials using cross-linkable, hyperbranched chromophore-containing oligomers as a macromolecular dopant. Journal of the American Chemical Society 2005;127(7):2060–1.
[59] Tsutsumi N, Moridhima M, Sakai W. Nonlinear optical (NLO) polymers. 3. NLO polyimide with dipole moments aligned transverse to the imide linkage. Macromolecules 1998;31(22):7764–9.
[60] Clays K, Coe BJ. Design strategies versus limiting theory for engineering large second-order nonlinear optical polarizabilities in charged organic molecules. Chemistry of Materials 2003;15(3):642–8.
[61] Barto RR, Frank CW, Bedworth PV, Taylor RE, Anderson WW, Ermer S, et al. Bonding and molecular environment effects on near-infrared optical absorption behavior in nonlinear optical monoazo chromophore–polymer materials. Macromolecules 2006;39(22):7566–77.
[62] Chen CP, Huang GS, Jeng RJ, Chou CC, Su WC, Chang HL. Low loss second-order non-linear optical crosslinked polymers based on a phosphorus-containing maleimide. Polymers for Advanced Technologies 2004;15(10):587–92.
[63] Kim E, Cho SY, Yeu DM, Shin SY. Low optical loss perfluorinated methacrylates for a single-mode polymer waveguide. Chemistry of Materials 2005;17(5):962–6.